

Thermodynamics of finite magnetic two-isomer systems

Peter Borrmann, Heinrich Stamerjohanns,^{a)} and Eberhard R. Hilf
Department of Physics of the University Oldenburg, D-26111 Oldenburg, Germany

Philippe Jund,^{b)} Seong Gon Kim,^{c)} and David Tománek
Department of Physics and Astronomy, Michigan State University, East Lansing, Michigan 48824-1116

(Received 28 June 1999; accepted 23 September 1999)

We use Monte Carlo simulations to investigate the thermodynamical behavior of aggregates consisting of few superparamagnetic particles in a colloidal suspension. The potential energy surface of this classical two-isomer system with a stable and a metastable “ring” and “chain” configuration is tunable by an external magnetic field and temperature. We determine the complex “phase diagram” of this system and analyze thermodynamically the nature of the transition between the ring and the chain “phase.” © 1999 American Institute of Physics.
 [S0021-9606(99)51747-9]

I. INTRODUCTION

With progressing miniaturization of devices,¹ there is a growing interest in the thermodynamical behavior of finite-size systems. A central question in this respect is, whether small systems can exhibit well-defined transitions that could be interpreted as a signature of phase transitions which, strictly speaking, are well defined only in infinite systems.² So far, reproducible features of the specific heat have been interpreted as indicators of “melting” transitions in small rare gas clusters.^{3,4} While most of the computational studies of cluster thermodynamics have considered only one external variable, namely either the temperature or the energy, there is only one study by Cheng *et al.*,⁵ where the pressure p entered as a second variable.

Here, we investigate the thermodynamical behavior of a finite system which is also controlled by *two* external variables, namely the temperature T and the magnetic field B_{ext} . The system of interest consists of few near-spherical, superparamagnetic particles with a diameter of $\approx 10\text{--}500$ Å in a colloidal suspension. Such systems, covered by a thin surfactant layer, are readily available in macroscopic quantities, are called ferrofluids, and are known to form complex labyrinth⁶ or branched structures⁷ as many-particle systems, whereas the only stable isomers for systems with few particles ($N < 14$) are the “ring” and the “chain.”⁸

The existence of two environmental variables, yet still only two isomer states, gives rise to a rich thermodynamic behavior, as compared to that of other small clusters such as the noble gas clusters.^{3,4} This classical, externally tunable finite two-isomer system is quite different from finite spin lattices, where magnetic interactions between fixed sites are parametrized.^{2,9} The magnetic tops in our system are free to move in three-dimensional space and their magnetic dipole–

dipole interaction has a nontrivial spatial dependence.

We will show that the system exhibits a phase transition between *two* ordered phases, one magnetic and the other nonmagnetic, as well as phase transitions between these ordered phases and a disordered phase. Whereas the system is not susceptible to small magnetic fields, it shows a strong paramagnetic response when exposed to larger magnetic fields.

II. MODEL

Our model system consists of six spherical magnetite particles with a diameter of $\sigma = 200$ Å and a large permanent magnetic moment $\mu_0 = 1.68 \times 10^5 \mu_B$. The potential energy E_p of this system in the external field \mathbf{B}_{ext} consists of the interaction between each particle i and the applied field, given by $u_i = -\boldsymbol{\mu}_i \times \mathbf{B}_{\text{ext}}$, and the pair-wise interaction between the particles i and j , given by⁸

$$u_{ij} = (\mu_0^2 / r_{ij}^3) [\hat{\boldsymbol{\mu}}_i \times \hat{\boldsymbol{\mu}}_j - 3(\hat{\boldsymbol{\mu}}_i \times \hat{\mathbf{r}}_{ij})(\hat{\boldsymbol{\mu}}_j \times \hat{\mathbf{r}}_{ij})] + \epsilon \left[\exp\left(-\frac{r_{ij} - \sigma}{\rho}\right) - \exp\left(-\frac{r_{ij} + \sigma}{2\rho}\right) \right]. \quad (1)$$

The first term in Eq. (1) is the magnetic dipole–dipole interaction energy. The second term describes a nonmagnetic interaction between the surfactant covered tops in a ferrofluid that is repulsive at short range and attractive at long range.⁷ We note that the most significant part of this interaction, which we describe by a Morse-type potential with parameters $\epsilon = 0.121$ eV and $\rho = 2.5$ Å, is the short-range repulsion, since even at equilibrium distance the attractive part does not exceed 10% of the dipole–dipole attraction. The thermal equilibrium structures of small clusters are either rings or chains, which can be easily distinguished by their mean magnetic moment $\langle \mu \rangle$.

III. NUMERICAL METHOD

The canonical partition function, from which all thermodynamical quantities can be derived, is given by

^{a)}Author to whom correspondence should be addressed. Electronic mail: stamer@uni-oldenburg.de

^{b)}Present address: Laboratoire des Verres, Université de Montpellier 2, Case 069 - Place Eugene Bataillon, F-34095 Montpellier Cedex 5, France.

^{c)}Present address: Code 6690, Complex Systems Theory Branch, Naval Research Laboratory, Washington, DC 20375-5320.

$$Z(B_{\text{ext}}, T) = (2\pi\beta)^{-6N/2} \int \left[\prod_{i=1}^N d\mathbf{x}_i d\phi_i d\theta_i d\psi_i \right] \times \exp\left(-\beta\left(\sum_{i<j}^N u_{ij} - \sum_i^N \mu_{i,z} B_{\text{ext}}\right)\right), \quad (2)$$

where $\beta = (k_B T)^{-1}$ and where the field \mathbf{B}_{ext} is aligned with the z -axis. The pre-exponential factor addresses the fact that each particle has three rotational and three center-of-mass degrees of freedom. The key quantities are the formation enthalpy of the isolated system, $E^* = \sum_{i<j} u_{ij} = E_p + \mu_z B_{\text{ext}}$, and the z -component of the total magnetic moment of the aggregate, μ_z , both of which are functions of T and B_{ext} . E^* is the appropriate thermodynamic potential describing the present system; its definition is analogous to the enthalpy of a (p,V,T)-ensemble.

We studied the thermodynamical behavior of the system in a set of 32 extensive Metropolis Monte Carlo simulations,¹⁰ each of which consisted of 6×10^9 steps. We used the multiple histogram method of Ferrenberg *et al.*^{11,12} to combine the results of all simulations and to calculate the normalized density of states $\rho(E^*, \mu_z)$ with a minimized statistical error.¹³ In order to cover the 6N-dimensional configuration space properly and to eliminate any potential dependencies on the starting configurations, we based our data analysis on simulations performed with B and T close to the ‘‘phase boundary’’ between rings and chains.

With the density of states $\rho(E^*, \mu_z)$ at hand, the partition function Z can be rewritten as

$$Z(B_{\text{ext}}, T) = (2\pi\beta)^{-6N/2} \int dE^* d\mu_z \rho(E^*, \mu_z) \times \exp(-\beta(E^* - \mu_z B_{\text{ext}})), \quad (3)$$

and the field- and temperature-dependence of the expectation value of any function $F(E^*, \mu_z)$ can be obtained from

$$\langle F(E^*, \mu_z; B_{\text{ext}}, T) \rangle = Z^{-1}(B_{\text{ext}}, T) \int d\mu_z \int dE^* F(E^*, \mu_z) \rho(E^*, \mu_z) \times \exp(-\beta(E^* - \mu_z B_{\text{ext}})).$$

IV. RESULTS

In order to obtain a rough idea of the stable and metastable states of the system, we plotted in Fig. 1 the probability of finding the aggregate in a state with potential energy E_p and total magnetic moment in the field direction μ_z . This is the projection of the probability to find the system in a specific state in the high-dimensional configuration space onto the (E_p, μ_z) subspace. High probability regions in this subspace indicate not only the energetic preference of the corresponding states, but also their entropic preference due to a large associated phase space volume.

Rings always have an absolute magnetic moment $|\mu/\mu^{\text{max}}|$ that is close to zero. Consequently, the z -component of the magnetic moment of rings is also near zero, as seen in Fig. 1. Even though the absolute magnetic moment $|\mu/\mu^{\text{max}}|$ of chains is close to 1, these aggregates

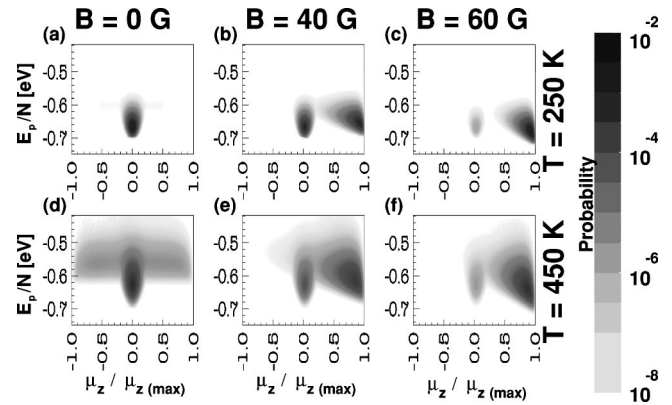


FIG. 1. Monte Carlo results for the probability to find an aggregate in a state with its magnetic moment in the field direction μ_z and potential energy E_p . The individual contour plots show our results for the temperature $T = 250$ K at the field values (a) $B_{\text{ext}} = 0$ G, (b) $B_{\text{ext}} = 40$ G, (c) $B_{\text{ext}} = 60$ G, and $T = 450$ K at the field values, (d) $B_{\text{ext}} = 0$ G, (e) $B_{\text{ext}} = 40$ G, (f) $B_{\text{ext}} = 60$ G.

cannot be distinguished easily from rings in the absence of a field. In the zero field, chains have no orientational preference and the z -component of their magnetic moment μ_z/μ_z^{max} averages to zero. Of course, this is not a serious complication within our simulations but in an experimental situation the measurement of one component of the magnetic moment μ would not be sufficient to determine the dominant structure of an ensemble of clusters.

Chains—unlike rings—do align with a nonzero magnetic field and, especially at low temperatures, show a magnetic moment $\mu_z/\mu_z^{\text{max}} \approx 1$ in the field direction.

The relative stability of an aggregate is reflected in its potential energy E_p . We find E_p to increase (corresponding to decreasing stability) with increasing temperature. On the other hand, applying a magnetic field destabilizes rings in favor of field-aligned chains. With increasing field, chains are confined to a gradually decreasing fraction of the configurational space which sharpens their distribution in the (E_p, μ_z) subspace, as seen when comparing Figs. 1(a)–1(c) and Figs. 1(d)–1(f).

Under all conditions, we find two more or less pronounced local maxima in the probability distribution P , corresponding to a ring with $0 \leq \mu_z/\mu_z^{\text{max}} \ll 1$, and a chain with $0 \leq \mu_z/\mu_z^{\text{max}} \leq 1$. At zero field we observe a predominant occupation of the more stable ring state. Due to the relatively small energy difference with respect to the less favorable chain $\Delta E_p^{\text{cr}}/N = (E_p^{\text{chain}} - E_p^{\text{ring}})/N = 0.06$ eV, both states become more evenly occupied at higher temperatures. At fields as low as $B_{\text{ext}} = 40$ G, the energy difference between chains and rings drops significantly to $\Delta E_p^{\text{cr}}/N = 0.02$ eV. As seen in Fig. 1(b), this results in an equal occupation of both states even at low temperatures. At the much higher field value $B_{\text{ext}} = 60$ G, chains are favored with respect to the rings by a considerable amount of energy $\Delta E_p^{\text{cr}}/N = -0.2$ eV. This strongly suppresses the occurrence of rings, as seen in Figs. 1(c) and 1(f).

A first-order phase transition in an infinite system can be identified by a discontinuous change of the energy at the critical point.

In corresponding finite systems, this critical point ex-

pands to a “critical region.” Even though the energy changes continuously in the finite system, such a transition may still be classified as a first-order transition or a higher-order phase transition, like in the work of Proykova and Berry,¹⁴ due to its physical similarity to those in infinite systems. We investigated the nature of the transition in our system by inspecting the temperature dependence of the bimodal distribution, shown in Fig. 1, following a procedure outlined in Refs. 15–17. This analysis revealed the transition between rings and chains, which is a transition between two ordered phases being “first-order like”. We have to emphasize that this classification is drawn by analogy. Unlike other small systems like those considered by Cheng *et al.*,⁵ it does not make sense to ask if the “transition” observed would become a true first-order phase transition in the limit of large particle numbers. Here, we discuss explicitly a finite magnetic two-isomer system. With increasing system size the number of different isomers (complex labyrinth⁶ or branched structures⁷) will increase dramatically and features like the bimodal probability distribution will probably disappear. For this reason, methods like finite-size scaling cannot be applied for the system under consideration. The ring–chain transition observed for small ferrofluid clusters will definitely disappear for larger clusters. Thus, the *traditional* way to classify phase transitions by studying the behavior of the probability distribution as a function of N cannot be used here. There is also some experimental evidence that this way might not be suitable for other clusters types, e.g., sodium clusters which exhibit a transition from molecular-like to jellium-like clusters with increasing particle number.¹⁸ In such cases it is easy to imagine that the type of phase transition as extracted from the probability function changes from first to higher order by going from N to $N + 1$ or $N - 1$. The phase behavior of a small sodium cluster might be more similar to that of a large argon cluster than to that of a large sodium cluster. There is apparently a growing need for a systematic definition of phase transitions in finite systems. Recently, an attempt to solve this problem has been made by analyzing the distribution of zeros of the canonical partition function in the complex temperature plane.¹⁹

Figure 1 shows not only the stable and metastable states under the given conditions, but also the states found along the preferential transition pathway between a ring and a chain in the projected (E_p, μ_z) subspace. During this transition each aggregate must undergo a *continuous* change of E_p and μ_z . The favored transition pathways are then associated with high-probability trajectories in the (E_p, μ_z) subspace. The value of the activation barrier ΔE_p^{act} is then given by the smallest increase of E_p along the optimum transition path which connects the stable and metastable ring and chain islands. In our simulations we found that the activation barrier always occurred at $\mu_z/\mu_z^{\text{max}} \approx 0.22$. Consequently, we concluded that the field dependence of the activation energy follows the expression $\Delta E_p^{\text{act}}(B_{\text{ext}}) = \Delta E_p^{\text{act}}(B_{\text{ext}} = 0) - 0.22 \mu_z^{\text{max}} B_{\text{ext}}$.

In order to quantitatively describe the phase transitions occurring in this system, we focused our attention on the specific heat and the magnetic susceptibility. The specific heat per particle in a canonical ensemble is given by c_B

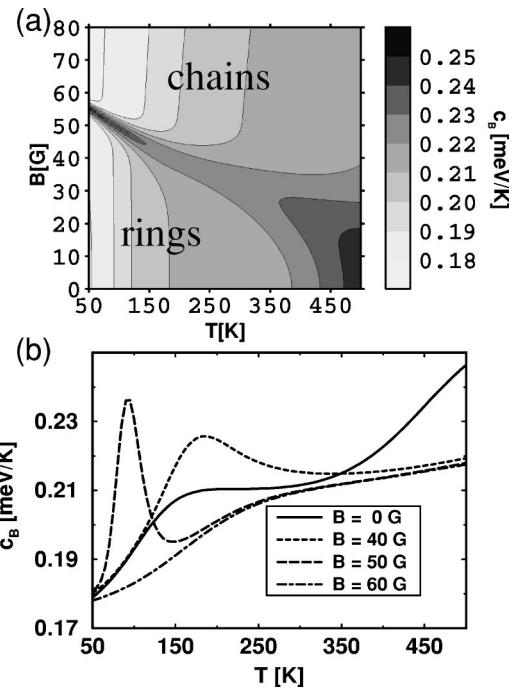


FIG. 2. Specific heat per particle c_B of the system as a function of temperature T and the external magnetic field B_{ext} . Results for the entire temperature and field range investigated here are presented as a contour plot in (a). The temperature dependence of c_B for selected values of B_{ext} is presented in (b).

$= d\langle E/N \rangle / dT$, where the total energy is given by $E = (6/2)Nk_B T + E_p$. Correspondingly, we define the magnetic susceptibility per particle as $\chi = d\langle \mu_z / N \rangle / dB_{\text{ext}}$. These response functions are related to the fluctuations of E_p and μ_z by

$$c_B = \left[\frac{6N}{2} k_B + k_B \beta^2 (\langle E^2 \rangle - \langle E \rangle^2) \right] / N, \quad (4)$$

$$\chi = [\beta (\langle \mu_z^2 \rangle - \langle \mu_z \rangle^2)] / N. \quad (5)$$

As already mentioned, transitions in finite systems are gradual.² Still, it makes physical sense to compare them to phase transitions in infinite systems. There, first-order phase transitions are associated with a diverging specific heat at the phase boundary. In the $T - B_{\text{ext}}$ “phase diagram” in Fig. 2(a), a well-defined yet not sharp “crest line” separates the ring and the chain phase. Similar phase diagrams, albeit for nonmagnetic systems, have been discussed in Refs. 3 and 20. Our results illustrate how the critical magnetic field for the ring–chain transition decreases with increasing temperature. At high temperatures, the “line” separating the phases broadens significantly into a region where rings and chains coexist.

The line plot in Fig. 2(b) is the respective constant-field cut through the contour plot in Fig. 2(a). As can be seen in Fig. 2(b), there is no transition from chains to rings, indicated by a peak in c_B at fields exceeding 50 G which is close to the critical field value at which chains become favored over rings at zero temperature. At fields $B_{\text{ext}} \ll 40$ G, on the other hand, there is no region where chains would be thermodynamically preferred over the rings, and we observe

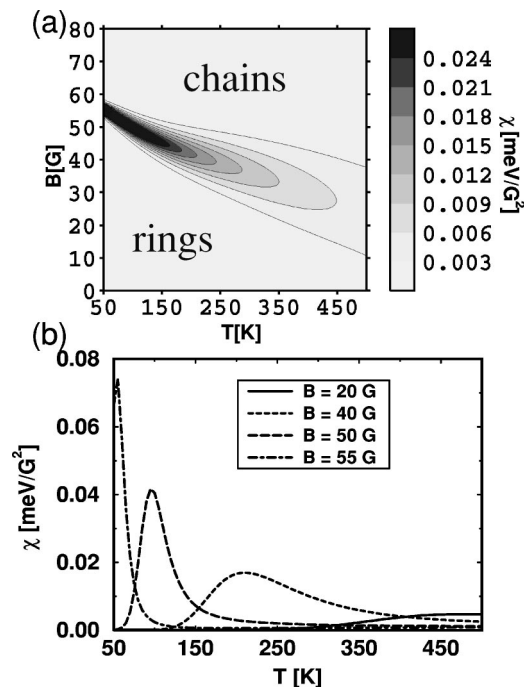


FIG. 3. Magnetic susceptibility per particle χ of the system as a function of temperature T and the external magnetic field B_{ext} . Results for the entire temperature and field range investigated here are presented as a contour plot in (a). The temperature dependence of χ for selected values of B_{ext} is presented in (b).

only a gradual transition from the ring phase into the coexistence region with increasing temperature. The specific heat behavior at zero field resembles that of a small system with a gradual *melting* transition close to 150 K and an onset of disorder at about 350 K.²¹ As seen in Fig. 2(b), the critical temperature and the width of the transition region can be externally tuned by the second thermodynamical variable, the external magnetic field B_{ext} .

Figure 3 displays the magnetic susceptibility χ , another prominent indicator of phase transitions in magnetic systems, as a function of T and B_{ext} . Like the specific heat in Fig. 2(a), the crest line in χ separates the chain phase from the ring phase in this T – B_{ext} phase diagram. Moreover, Fig. 3 reveals the fundamentally different magnetic character of these phases. Whereas the system is nonmagnetic in the ring phase found below 40 G, it behaves like a ferromagnet consisting of Langevin paramagnets in the chain phase at higher fields. The transition between these states is again gradual. The line plot in Fig. 3(b) is the respective constant-field cut through the contour plot in Fig. 3(a). When the system is in the chain phase, it behaves like a paramagnet obeying the Curie–Weiss law, as can be seen in Fig. 3(b).²²

At relatively low temperatures, where the aggregates are intact, the expectation value of the magnetic moment first increases with increasing magnetic fields. This is due to the gradual conversion from nonmagnetic rings to paramagnetic chains. According to Fig. 3(b), this uncommon behavior persists up to $T = 200$ K at $B_{\text{ext}} = 40$ G. This trend is reversed at higher temperatures, where all aggregates eventually fragment into single paramagnetic tops. In this temperature range the magnetic moment as well as the susceptibility decrease

with increasing temperature. Snapshots from our simulations at temperatures in the melting region indicate that rings and chains break up to form a number of different isomers. Single particles leave the chain and ring structures and attach at arbitrary positions. We interpret this as the onset of disordering or melting. For computational reasons the dissociation process has not been studied in detail.

Since the transition probability between both states is extremely low at low temperatures and fields, magnetically distinguishable metastable states can be frozen. A chain configuration, which is metastable in zero field, can be prepared by first annealing the system to $T \geq 350$ K and subsequent quenching in a strong field. Similarly a frozen-in ring configuration is unlikely to transform to a chain at low temperatures, unless exposed to very large fields. Thus, the above-described phase diagrams can be used to externally manipulate the self-assembly of magnetic nanostructures.

In conclusion, we have studied the thermodynamic behavior of a finite two-isomer system, which is externally tunable by two independent variables, namely the temperature and the magnetic field. Much of the behavior encountered in this system such as transitions between different states has a well-defined counterpart in infinite systems. The reason for the encountered richness of the thermodynamic and magnetic properties is the relative ease of structural transformations which is typical for finite systems. Consequently, we expect other finite magnetic systems, e.g., small transition metal clusters, where a small number of structural isomers with substantially different magnetic moments could coexist,²³ to follow this behavior. Moreover, we expect that our results can also be transferred to nanocrystalline material, such as magnetic clusters encapsulated in the supercages of zeolites, which will likely retain some of the intriguing properties of the isolated finite systems.

¹K. Gabriel, *Sci. Am.* **273**(3), 150 (1995).

²T. Hill, *Thermodynamics of Small Systems* (Parts I and II) (W.A. Benjamin, New York, 1963 and 1964).

³R. E. Kunz and R. S. Berry, *Phys. Rev. Lett.* **71**, 3987 (1993); D. J. Wales and R. S. Berry, *ibid.* **73**, 2875 (1994).

⁴P. Borrmann, *COMMAT* **2**, 583 (1994); G. Franke, E. R. Hilf, and P. Borrmann, *J. Chem. Phys.* **98**, 3496 (1993).

⁵H.-P. Cheng, X. Li, R. L. Whetten, and R. S. Berry, *Phys. Rev. A* **46**, 791 (1992).

⁶A. J. Dickstein *et al.*, *Science* **261**, 1012 (1993).

⁷H. Wang, Y. Zhu, C. Boyd, W. Luo, A. Cebers, and R. E. Rosensweig, *Phys. Rev. Lett.* **72**, 1929 (1994).

⁸P. Jund, S. G. Kim, D. Tománek, and J. Hetherington, *Phys. Rev. Lett.* **74**, 3049 (1995).

⁹A. E. Ferdinand and M. E. Fisher, *Phys. Rev.* **185**, 832 (1969).

¹⁰N. Metropolis, A. Rosenbluth, M. N. Rosenbluth, A. H. Teller, and E. Teller, *J. Chem. Phys.* **21**, 1087 (1953).

¹¹A. M. Ferrenberg and R. H. Swendsen, *Phys. Rev. Lett.* **61**, 2635 (1988).

¹²A. M. Ferrenberg and R. H. Swendsen, *Phys. Rev. Lett.* **63**, 1195 (1989).

¹³We extended the Ferrenberg analysis in a straightforward way to deal with a two-dimensional density of states.

¹⁴A. Proykova and R. S. Berry, *Z. Phys. D: At., Mol. Clusters* **40**, 215 (1997).

¹⁵M. Glosli and J. Plischke, *Can. J. Phys.* **61**, 1515 (1983).

¹⁶O. G. Mouritsen, *Computer Studies of Phase Transitions and Critical Phenomena* (Springer, Berlin, 1984).

¹⁷Y. Zhou, C. K. Hall, and M. Karplus, *Phys. Rev. Lett.* **77**, 2822 (1996).

¹⁸C. Ellert, M. Schmidt, T. Reiners, and H. Haberland, *Z. Phys. D: At., Mol. Clusters* **39**, 317 (1997).

¹⁹P. Borrmann and O. Muelken, eprint: cond-mat/9909184 1999.

²⁰S. Sugano and S. Sawada, *Z. Phys. D: At., Mol. Clusters* **12**, 189 (1989).

²¹R. S. Berry, J. Jellinek, and G. Natanson, *Chem. Phys. Lett.* **107**, 227 (1984); G. Natanson, F. Amar, and R. S. Berry, *J. Chem. Phys.* **78**, 399 (1983).

²²Our numerical approach did not allow us to investigate the temperature

region below 50 K. The onset of the Curie–Weiss behavior, indicated by a maximum in χ at nonzero temperature, can be seen whenever the system is in the chain phase.

²³P. Borrmann, B. Diekmann, E. R. Hilf, and D. Tománek, *Surf. Rev. Lett.* **3**, 103 (1996).